Acta Ophthalmologica

Acta Ophthalmologica 2012

Scanning laser ophthalmoscopy in the retromode in diabetic macular oedema

Stela Vujosevic,[1] Barbara Trento,[2] Elisa Bottega,[2] Francesca Urban,[2] Elisabetta Pilotto[2] and Edoardo Midena[1,2]

[1]G.B Bietti Eye Foundation, IRCCS, Rome, Italy
[2]Department of Ophthalmology, University of Padova, Padova, Italy

ABSTRACT.

Purpose: **To determine the validity of scanning laser ophthalmoscopy in the retromode (RM-SLO) versus other imaging modalities in the diagnosis of diabetic macular oedema (DME).**

Methods: **Two hundred and sixty-three eyes were examined. Inclusion criteria were any stage of untreated or treated diabetic retinopathy and four imaging modalities of the macula carried out on the same day: time domain optical coherence tomography (OCT), fundus autofluorescence (FAF), RM-SLO and fluorescein angiography (FA). Two masked retinal specialists independently graded all images. Agreement between RM-SLO and OCT, FA and FAF in evaluating the presence and patterns of DME was evaluated by kappa statistics, sensitivity, specificity, observed proportional agreement, and proportional agreement in positive and negative cases.**

Results: **The agreement in evaluating the presence/absence of DME between RM-SLO and OCT, FA and FAF was good: κ = 0.73 (confidence interval; CI, 0.64–0.83), κ = 0.71 (CI, 0.61–0.81) and κ = 0.73 (CI, 0.63–0.83), respectively. The agreement in evaluating cystoid pattern of DME was almost perfect between RM-SLO and OCT, RM-SLO and FA, κ > 0.8; and good between RM-SLO and FAF, κ > 0.7. The agreement in evaluating the presence/absence of subfoveal neuroretinal was almost perfect between RM-SLO and OCT (κ = 0.83; 95% CI, 0.70–0.96). Subfoveal neuroretinal detachment did not show any specific pattern on FA or FAF. Sensitivity and specificity of RM-SLO in evaluating DME was 97.7% and 71.9% versus OCT, 97.4% and 68.1% versus FA and 96.1% and 73.3% versus FAF. Retinal thickness of 233 μm represented the cut-off value to define DME by RM-SLO.**

Conclusions: **The combined use of non-invasive imaging techniques can improve the diagnostic interpretation of different aspects of DME.**

Key words: diabetic macular oedema – fluorescein angiography – fundus autofluorescence – optical coherence tomography – retromode – scanning laser ophthalmoscopy

Acta Ophthalmol. 2012: 90: e374–e380

doi: 10.1111/j.1755-3768.2012.02410.x

Introduction

Diabetic macular oedema (DME) is the major cause of visual loss in patients with diabetes (Klein et al. 1998). Although DME is a treatable disease, local treatment has still unpredictable outcome (Beck et al. 2009). This is probably caused by the existence of different DME phenotypes, requiring an individual therapeutic approach (Ehrlich et al. 2010). Slit lamp biomicroscopy, fluorescein angiography (FA) and optical coherence tomography (OCT) remain the mainstay in the diagnosis and follow-up of this disease. Recently, fundus autofluorescence (FAF), a non-invasive imaging technique, has been proposed in the evaluation of DME (Pece et al. 2009; Vujosevic et al. 2011). Diabetic macular oedema with increased foveal autofluorescence showed decreased retinal sensitivity (determined by microperimetry) compared to DME with normal foveal autofluorescence, indicating that the function of the neurosensory retina significantly deteriorates when FAF increases (Vujosevic et al. 2011). Therefore, non-invasive imaging techniques may be useful to better identify different DME characteristics and possibly phenotypes. Although OCT has added relevant information in quantitative and qualitative evaluation of DME, it fails to give immediate information about the extension of oedema (Ohkoshi et al. 2010). Fluorescein angiography, previously routinely

used in DME diagnosis, is an invasive technique, and its use in clinical practice is significantly decreasing (Browning et al. 2008). Scanning laser ophthalmoscopy in the retromode [Retromode Scanning Laser Ophthalmoscopy (RM-SLO)] is a non-invasive imaging tool, which enables an easy visualization of deep retinal structures by using an infrared laser light (Yamamoto et al. 2008, 2010; Ohkoshi et al. 2010; Acton et al. 2011). It uses a central stop, which blocks directly reflected light, while collecting laterally oriented scattered light. As a consequence, pseudo-3-dimensional images of the retina are obtained. Retromode Scanning Laser Ophthalmoscopy has been used for the visualization of cystoid macular oedema of different origin, and drusen in age-related maculopathy (Yamamoto et al. 2008, 2010; Ohkoshi et al. 2010; Acton et al. 2011). In DME, it has been recently used for the visualization of subthreshold micropulse diode laser treatment spots (Ohkoshi et al. 2010). A systematic evaluation on RM-SLO in patients with diabetes has never been performed before. Moreover, any new diagnostic technique needs a comparative study versus more standardized examinations to validate its use in the classification (and management) of any specific disorder. The purpose of this study was to evaluate RM-SLO in DME and to compare it to OCT, FA and FAF.

Materials and Methods

A total of 263 eyes of 137 consecutive patients with diabetes were included in this study. All patients were recruited from the diabetic retinopathy (DR) clinics from March to August 2009. Inclusion criteria were men or women with type 1 or 2 diabetes mellitus (DM); any stage of untreated or treated DR; and no significant media opacities and patients having all four imaging modalities: OCT, FAF, fluorescein angiography (FA) and RM-SLO performed on the same day. All patients underwent slit lamp fundus examination of the macula using 60 dioptres lens. A written consent form was obtained from all patients as well as the approval from our institutional review board. The study was conducted in accordance with the tenets of the Declaration of Helsinki.

Study procedures

Fundus examination

Stereoscopic slit lamp fundus examination of the macula was performed with 60 dioptres lens by two retinal specialists, independently.

Optical coherence tomography

Optical coherence tomography scanning was performed on the Stratus OCT TM scanner (Zeiss Humphrey Instruments, Carl Zeiss Meditec GmbH, Oberkochen, Germany) with the 4.1 (0052) version software. The scanning protocol used for this study was 'fast macular thickness' programme that creates a retinal map algorithm consisting in six radiating cross-sectional scans, each one 6 mm in length produces a circular plot in which the foveal zone is the central circular zone 1.00 mm in diameter. For the purpose of this study, retinal thickness in the central 1 mm was used as the OCT measurement of foveal thickness (central retinal thickness). Macular oedema was assigned if central retinal thickness was higher than 230 μm (Virgili et al. 2007). Moreover, four additional line scans, 5 mm length, were performed centred on the fovea at 0°, 45°, 90° and 135°. These images were saved on hard disk and graded for oedema pattern classification, according to the classification proposed by Otani et al. (1999): cystoid pattern, sponge-like pattern (diffuse) and serous neuro-retinal detachment (SND).

Fundus autofluorescence

Fundus autofluorescence was recorded with a confocal scanning laser ophthalmoscope (Heidelberg Retinal Angiograph, HRA 2; Heidelberg Engineering, Heidelberg, Germany) using blue wavelength (solid-pumped laser; 488 nm) for excitation, whereas emitted light is detected above 500 nm because of a barrier filter. The optical and technical principles of the HRA have been previously described in detail (Bartsch et al. 1995; Holz et al. 1999). To amplify the autofluorescence signal of the final image, 15 acquired images were aligned, and a mean one was calculated from these, after detection and correction of eye movements were performed by image analysis software. Digital images were saved on hard disk for further analysis and processing. Fundus autofluorescence images were graded for different foveal patterns (normal, single spot increased and multiple spots increased) (Vujosevic et al. 2011). Fundus autofluorescence images were also graded for the presence/absence of decreased/increased autofluorescence in the macula (Vujosevic et al. 2010).

Fluorescein angiography

Fluorescein angiography of ETDRS field 2 was taken in all patients after an adequate dilatation by a trained photographer using TOPCON TRC 50IA 35° fundus camera (Topcon, Tokyo, Japan) and saved in JPEG format. Late-phase FA images of the macula were graded for the presence of fluorescein leakage and pattern of leakage (cystoid and non-cystoid). In case of cystoid leakage, its pattern (one or multiple cysts) was also evaluated.

Scanning laser ophthalmoscopy in the retromode

Retromode Scanning Laser Ophthalmoscopy images were obtained with F-10 SLO (Nidek Co, Gamagori, Japan). F-10 is a scanning laser ophthalmoscope that uses four different wavelengths (blue, green, red and infrared). The infrared laser is set at 790 nm. Moreover, F-10 contains eight different apertures (five confocal apertures and three apertures with a central stop) and five stops. To obtain a RM-SLO image, a central stop and a laterally oriented oval-shaped opening is used, from both the right and left side. Retromode Scanning Laser Ophthalmoscopy differs from the previously reported SLO used in the indirect (dark field) mode, with an infrared laser, because both a central stop and a full ring aperture were used. Using this system, a relatively large amount of multiply scattered light is collected (Elsner et al. 1992, 1996; Remky et al. 1999; Yamamoto et al. 2010). In contrast, RM-SLO uses a modified central stop. The opening of the ring aperture is further restricted and is laterally deviated from the confocal light path. In this way, scattered light from just one direction is collected, and shadows to highlight objects are obtained by blocking the reflected light from the other direction (Ohkoshi et al. 2010).

Therefore, RM-SLO creates pseudo-3-dimensional images and allows for deep retinal structure evaluation with high contrast. Retromode Scanning Laser Ophthalmoscopy images were graded for the presence/absence of macular oedema. Presence/absence of cysts was also analysed. If cysts were present, their number was quantified (one cyst or multiple cysts).

All four types of imaging modalities (RM-SLO, OCT, FA and FAF) were graded for the presence/absence of macular oedema, pattern of DME [cystoid, sponge-like/diffuse and the presence of subfoveal neuroretinal detachment (SND)]. Microaneurysms were also evaluated on SLO-RM and FA. Two retinal specialists trained in imaging grading, independently graded, in a masked fashion, all images on a 17-inch monitor dedicated to DR screening (SV and EP). In case of disagreement, adjudication was given by the third party (EM).

Statistical methods

Sample size

A population value of kappa higher than 0.60 was considered clinically 'acceptable' for the aims of the study. The hypothesis that significant reliability index kappa is higher than 0.60 when the expected value is 0.80 and the proportion of positive ratings made using dichotomous classification of DME (present/absent) is 80% was verified according to a two-tailed test with a = 0.05. The minimum sample size required to guarantee a statistical power of 80% is 242 (Elsner et al. 1992). The null hypothesis that kappa is not higher than 0.60 was maintained only if 0.60 was within the confidence interval.

Reliability indexes

The agreement between RM-SLO and other diagnostic methods (i.e. OCT, FA and FAF) in evaluating the presence of DME, DME patterns, as well as pattern of cystoid oedema was the principal reliability index of the study. Kappa statistic (κ), a measure of inter-method reliability that adjusts for agreement by chance, and its 95% confidence interval (CI) were calculated (Altman 1997; Sim & Wright 2005). Other indexes were also computed to improve the evaluation of obtained results. Such indexes were sensitivity (SE), specificity (SP), observed proportional agreement (P_0), proportional agreement in positive cases (P_{pos}) and proportional agreement in negative cases (P_{neg}).

Macular thickness cut-off between the presence and absence of oedema

The empirical receiver operating characteristic (ROC) curve (Fawcett 2006) was drawn to determine the macular thickness cut-off value that better discriminates between the presence and absence of DME. The area under the curve, which is the probability of ranking a positive case higher than a negative one, was computed as well. All statistical analyses were performed with SAS/STAT® 9.13 statistical package for Windows, SAS (Cary, NC, USA).

Results

Of 137 patients (263 eyes), 87 were males and 50 females. Twelve patients had type 1 (10.1%) and 107 patients (89.9%) type 2 diabetes mellitus (DM). Mean age of patients was 48.8 + 11.5 years (range, 28–64 years) and 66.6 + 8.1 years (range, 41–85 years) in types 1 and 2 DM, respectively. Mean duration of DM type 1 was 28.8 ± 11.9 years (range, 5–51 years) and 15.4 ± 8.8 years (range, 1–39 years) of DM type 2. Mean central macular thickness was 323.4 ± 125.2 μm (range, 154.0–884.0).

Classification by different methods (RM-SLO, OCT, FA and FAF) of DME pattern (cystoid, diffuse and SND) and pattern of cystoid oedema (cystic and multicystic) is shown in Table 1. The agreement in evaluating the presence/absence of DME between RM-SLO and OCT, FA and FAF was good: κ = 0.73 (CI, 0.64–0.83), κ = 0.71 (CI, 0.61–0.81) and κ = 0.73 (CI, 0.63–0.83), respectively (Tables 2–4). The agreement in evaluating cystoid/diffuse pattern of DME was almost perfect between RM-SLO and OCT, RM-SLO and FA, $\kappa > 0.8$, and good between RM-SLO and FAF, $\kappa > 0.7$ (Tables 2–4). The agreement in evaluating the presence/absence of SND was almost perfect (κ = 0.83, 95% CI, 0.70–0.96) between RM-SLO and OCT (Table 2). Subfoveal neuroretinal detachment did not have any specific pattern on FA or FAF (Tables 3 and 4). The sensitivity and specificity of RM-SLO in evaluating macular oedema, defined as foveal thickening on OCT examination, were 97% and 71.9% versus OCT, 97.4% and 68.1% versus FA and 96.1% and 73.3% versus FAF, respectively (Tables 2–4). The highest sensitivity/specificity ratio for RM-SLO in evaluating DME was found at retinal thickness threshold of 233 μm, with a sensitivity of 89.1% and specificity of 78.8% (Fig. 1). Retromode Scanning Laser Ophthalmoscopy detected tiny localized elevations in 32 eyes, each one corresponding to leaking microaneurysms in FA (κ = 1, CI, 1) (data not shown).

Discussion

In this study, we found that SLO in the retromode and OCT show high and almost equivalent agreement in the evaluation of DME. Retromode Scanning Laser Ophthalmoscopy showed 97% sensitivity in detecting retinal thickening because of DME, defined as central retinal thickness >230 μm on Stratus OCT. Notwithstanding, the best correlation between

Table 1. Descriptive characteristics of 263 studied eyes by methods.

Characteristic	RM-SLO (%)	OCT (%)	FA (%)	FAF (%)
No oedema	52 (19.8)	64 (24.3)	69 (26.2)	60 (22.8)
Oedema	211 (80.2)	199 (75.7)	194 (73.8)	203 (77.2)
Diffuse	93 (44.1)	74 (37.2)	77 (39.7)	73 (36.0)
Cystoid	102 (48.3)	103 (51.8)	117 (60.3)	130 (64.0)
SND	16 (7.6)	22 (11.0)	NA	NA
Pattern of cystoid oedema, *n* (%)				
Cystic	31 (26.3)	31 (24.8)	27 (23.1)	34 (26.1)
Multicystic	87 (73.7)	94 (75.2)	90 (76.9)	96 (73.9)

RM-SLO = retromode scanning laser ophthalmoscopy; OCT = optical coherence tomography; FA = fluorescein angiography; FAF = fundus autofluorescence; SND = subfoveal neuroretinal detachment; *n* = number; NA = not applicable (because undetectable).

Table 2. Agreement between RM-SLO and OCT in evaluating different DME patterns.

Characteristic	Kappa (95% CI)	P_0	P_{pos}	P_{neg}	TP	Pos	SE	TN	Neg	SP
Oedema versus no oedema	0.74 (0.64–0.83)	90.9	94.1	79.3	193	199	97.0	46	64	71.9
DME pattern										
Diffuse	0.81 (0.73–0.89)	90.9	88.3	92.6	68	74	91.9	113	125	90.4
Cystoid	0.86 (0.79–0.93)	93.0	93.0	92.9	93	103	90.3	92	96	95.8
SND	0.83 (0.69–0.96)	97.0	84.2	98.3	16	22	72.7	177	177	100.0
Overall*	0.81 (0.74–0.88)									
Pattern of cystoids oedema										
Cystic	0.85 (0.74–0.96)	94.4	88.5	96.3	27	31	87.1	91	94	96.8
Multicystic	0.73 (0.61–0.86)	88.8	92.0	81.1	81	94	86.2	30	31	96.8
Overall†	0.70 (0.57–0.82)									

DME = diabetic macular oedema; RM-SLO = retromode scanning laser ophthalmoscopy; OCT = optical coherence tomography; P_0 = observed proportional agreement (%); P_{pos} = proportional agreement in positive cases (%); P_{neg} = proportional agreement in negative cases (%); TP = number of true positive cases (*n*) as classified by RM-SLO; Pos = number of positive cases (*n*) as classified by OCT; SE = sensitivity (%);TN = number of true negative cases (*n*) as classified by RM-SLO; Neg = number of negative cases (*n*) as classified by OCT; SND = subfoveal neuroretinal detachment; SP = specificity (%).
* Complete DME pattern: diffuse, cystoid and SND.
† Complete pattern of cystoid oedema: cystic and multicystic.

Table 3. Agreement between RM-SLO and FA in evaluating DME patterns.

Characteristic	Kappa (95% CI)	P_0	P_{pos}	P_{neg}	TP	Pos	SE	TN	Neg	SP
Oedema versus no oedema	0.71 (0.61–0.81)	89.7	93.3	77.7	189	194	97.4	47	69	68.1
DME pattern										
Diffuse	0.83 (0.75–0.91)	91.7	89.5	93.2	68	77	88.3	110	117	94.0
Cystoid	0.86 (0.79–0.93)	93.3	94.4	91.7	109	117	93.2	72	77	93.5
SND	NA									
Overall*	0.82 (0.74–0.90)									
Pattern of cystoid oedema										
Cystic	0.88 (0.78–0.98)	95.7	90.9	97.2	25	27	92.6	87	90	96.7
Multicystic	0.81 (0.69–0.92)	92.3	94.7	85.7	81	90	90.0	27	27	100.0
Overall†	0.77 (0.65–0.89)									

DME, diabetic macular oedema; RM-SLO, retromode scanning laser ophthalmoscopy; FA, fluorescein angiography; P_0 = observed proportional agreement (%); P_{pos} = proportional agreement in positive cases (%); P_{neg} = proportional agreement in negative cases (%); TP = number of true positive cases (*n*) as classified by RM; Pos = number of positive cases (*n*) as classified by FAG; SE = sensitivity (%);TN = number of true negative cases (*n*) as classified by RM; Neg = number of negative cases (*n*) as classified by FAG; SP = specificity (%); SND = subfoveal neuroretinal detachment; NA = not applicable because undetectable.
* Complete DME pattern: no oedema, diffuse, cystoid and SND.
† Complete pattern of cystoid oedema: cystic and multicystic.

Table 4. Agreement between retromode scanning laser ophthalmoscopy (RM-SLO) and fundus autofluorescence (FAF) in evaluating DME patterns.

Characteristic	Kappa (95% CI)	P_0	P_{pos}	P_{neg}	TP	Pos	SE	TN	Neg	SP
Oedema versus no oedema	0.73 (0.63–0.83)	90.9	94.2	78.6	195	203	96.1	44	60	73.3
DME pattern										
Diffuse	0.75 (0.65–0.84)	88.2	84.2	90.6	64	73	87.7	115	130	88.5
Cystoid	0.77 (0.69–0.86)	89.2	91.1	86.2	112	130	86.1	69	73	94.5
SND	NA									
Overall*	0.73 (0.64–0.82)									
Pattern of cystoids oedema										
Cystic	0.79 (0.66–0.91)	92.3	83.9	94.9	26	34	76.5	94	96	97.9
Multicystic	0.68 (0.54–0.81)	86.2	90.0	77.5	81	96	84.4	31	34	91.2
Overall†	0.62 (0.50–0.74)									

DME = diabetic macular oedema; RM-SLO = retromode scanning laser ophthalmoscopy; FAF = fundus autofluorescence; P_0 = observed proportional agreement (%); P_{pos} = proportional agreement in positive cases (%); P_{neg} = proportional agreement in negative cases (%); TP = number of true positive cases (*n*) as classified by RM; Pos = number of positive cases (*n*) as classified by AF; SE = sensitivity (%);TN = number of true negative cases (*n*) as classified by RM; Neg = number of negative cases (*n*) as classified by AF; SP = specificity (%); SND = subfoveal neuroretinal detachment; NA = not applicable because undetectable.
* Complete DME pattern: diffuse, cystoid and SND.
† Complete pattern of cystoid oedema: cystic and multicystic.

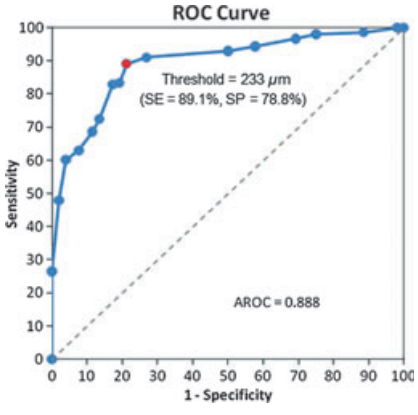

Fig. 1. Receiver Operating Characteristic (ROC) Curve. The empirical ROC curve showing the macular thickness cut-off value (233 μm) at which retromode SLO better discriminates between the presence and absence of diabetic macular oedema (sensitivity, SE = 89.1%; and specificity, SP = 78.8%). The area under the curve, which is the probability of ranking a positive case higher than a negative one, is 0.89.

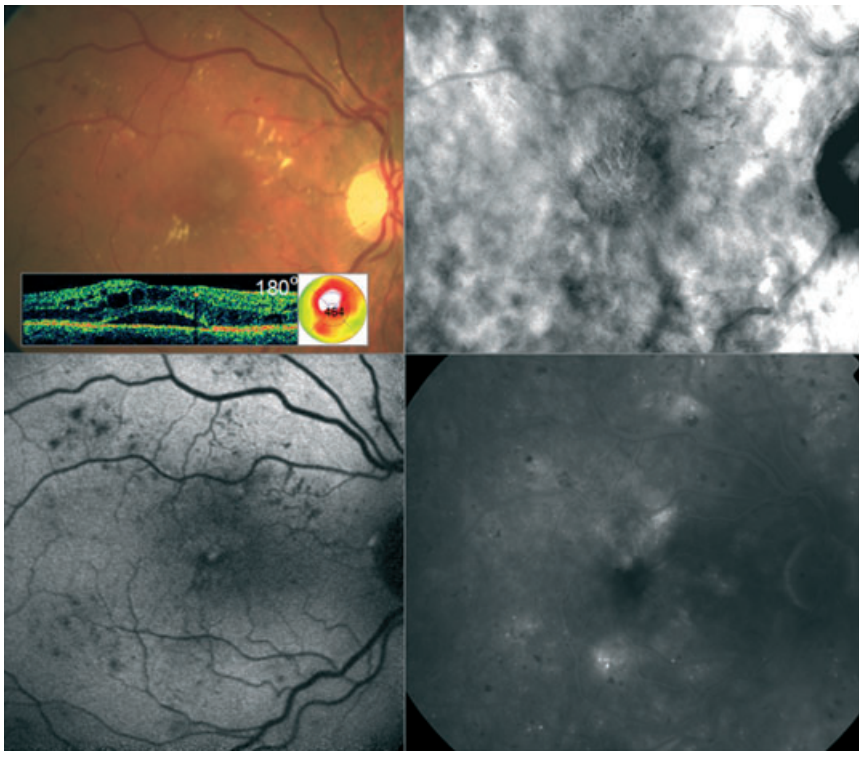

Fig. 2. Multimodal imaging in exudative diabetic macular oedema (DME) Fundus colour Photograph, optical coherence tomography (OCT) line scan (at 180°) and OCT map (Top Left). Retromode Scanning Laser Ophthalmoscopy (RM-SLO; top right), fundus autofluorescence (bottom left) and fluorescein angiography (bottom right) of the right eye of a patient with exudative cystoid DME with subfoveal neuroretinal detachment (SND). Retromode Scanning Laser Ophthalmoscopy nicely shows different intra-retinal cysts (small and large ones) overlying SND. Location and extension of SND and macular oedema are also easily evaluated.

sensitivity (89.1%) and specificity (78.8%) (obtained with ROC curve) was found at retinal thickness threshold of 233 μm. In a systematic review of published studies in which time domain OCT was used in detecting DME, Virgili et al. (2007) reported a sensitivity of 79% and specificity of 88% for central retinal thickness varying between 230 and 300 μm, although all reported studies were small case series. Brown et al. (2004) found the highest specificity (95.7%) at retinal thickness threshold of 300 μm using time domain OCT in 172 eyes. In the present study (including 263 eyes), moderately higher specificity (96.1%) was found with RM-SLO at the same retinal thickness threshold (300 μm). This central retinal thickness value was proposed as the cut-off value for laser photocoagulation in patients with DME (Virgili et al. 2007). Although OCT is considered the new gold standard in evaluating DME, RM-SLO also allows for an early detection of DME (Virgili et al. 2007). Moreover, the visualization of macular oedema location, and the extension of thickened area, is quite immediate by RM-SLO (Figs 2 and 3). Slightly lower agreement in evaluating the presence of DME was found between FA and RM-SLO. This might be explained by the fact that FA leakage does not always correspond to increased retinal thickness (Browning et al., 2008). When evaluating different DME patterns (diffuse and cystoid), all four imaging techniques showed good agreement. The best agreement was found between RM-SLO and FA in evaluating the presence of cystoid DME. In fact, both honeycomb and petaloid patterns of DME in FA were easily seen as cysts of different dimensions on RM-SLO (Figs 2 and 3). On the contrary, SND is detected just by OCT and RM-SLO. No specific patterns were found for SND on FA and FAF (Vujosevic et al. 2011). Optical coherence tomography better identifies SND thickness, whereas RM-SLO better shows SND extension and location. In the past, a research model of SLO, used in the so-called indirect mode with an infrared laser, was used in different retinal and subretinal disorders (Ikeda et al. 1998; Hartnett & Elsner 1996; Remky et al. 1999). The SLO indirect mode, consisting in a central stop and a full ring aperture, showed to be useful in visualizing alterations in deeper retinal layers and choroid, such as thickness changes because of atrophy, fluid accumulation, choroidal neovascularization or subretinal deposits (Elsner et al. 1996; Hartnett & Elsner 1996). Remky et al. (1999) used the same technique for the non-invasive detection and quantification of cysts in cystoid macular oedema of different origin. These authors described the cysts as holes with prominent edges, whereas superficial plane features were not visualized (Remky et al. 1999). Retromode Scanning Laser Ophthalmoscopy represents a modification and advancement of the indirect mode SLO, because it provides a repeatable and reliable higher contrast images because of the fully modified confocal aperture (the opening is positioned laterally from the confocal light path) (Elsner et al. 1992; Remky et al. 1999). Moreover, indirect mode SLO was just a research device, used for a limited period of time and without further studies. Currently, RM-SLO may be easily used in clinical practice.

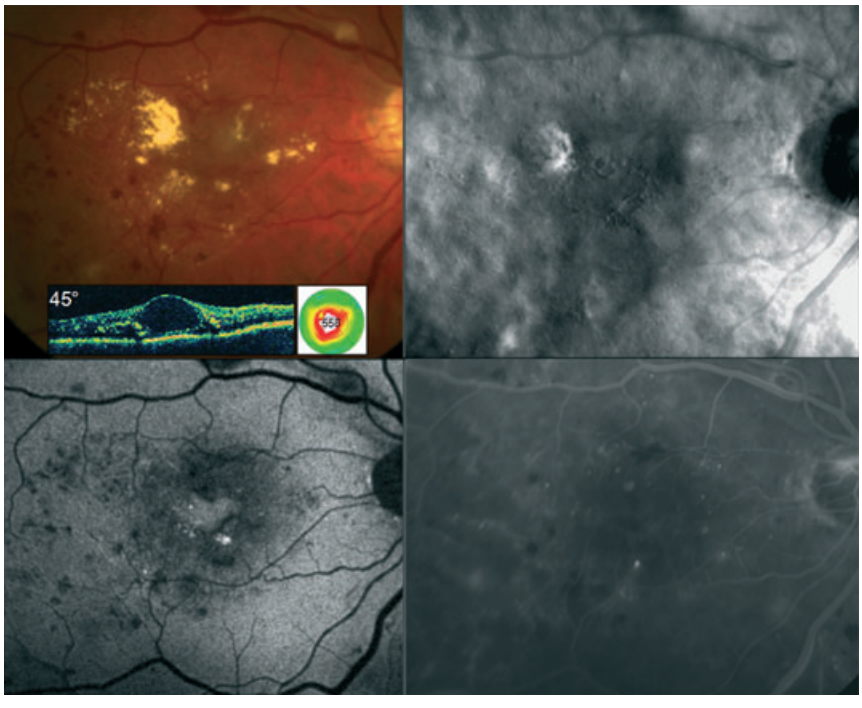

Fig. 3. Multimodal imaging in exudative diabetic macular oedema (DME). Fundus colour Photograph, optical coherence tomography (OCT) line scan (at 45°) and OCT map (top left). Retromode Scanning Laser Ophthalmoscopy (RM-SLO; top right), fundus autofluorescence (bottom left) and fluorescein angiography (bottom right) of the right eye of a patient with exudative cystoid DME. Retromode Scanning Laser Ophthalmoscopy nicely shows different intraretinal cysts (small and large ones) as well as location and extension of oedema.

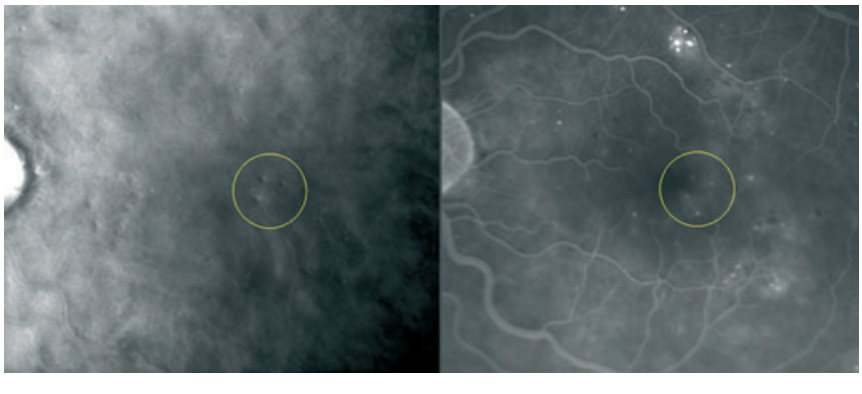

Fig. 4. Visualization of leaking microaneurysms on RM-SLO (left) and fluorescein angiography (right) of the same case showing diabetic macular oedema. Leaking microaneurysms (encircled in B) are detected as localized elevations (encircled in A) on RM-SLO.

Yamamoto et al. (2010) documented cystoid macular oedema of different origin with RM-SLO. These authors found that whereas OCT (both time and spectral domain machines) detects oedema well in the fovea, the quantification of its extension, obtained from longitudinal sections alone, remains difficult (Yamamoto et al. 2010). They also showed that even OCT en-face images, obtained by four different SD-OCTs, in eyes with cystoid macular oedema, detect a limited number of cystoid spaces. This depends on the location of cystoid spaces, which commonly encompass different retinal layers. Therefore, different en-face sections are needed to visualize all cystoid spaces as well as the extent of cystoid macular oedema (Yamamoto et al. 2010). Retromode Scanning Laser Ophthalmoscopy allows for clear visualization of each individual cystoid space, regardless of the layer of retina in which it occurs, because of scattered light that gives a shadow to the silhouetted cystoid space.

Cystoid macular oedema can also be easily detected by FAF (McBain et al. 2008; Vujosevic et al. 2011). In patients with diabetes, increased foveal FAF was found in 87% of eyes with cystoid DME and correlated to poorer visual function prognosis (Vujosevic et al. 2011). Therefore, RM-SLO and FAF might be included in the classification and evaluation of DME, because of the new information they offer as adjuncts to OCT. The classification of DME as focal or diffuse (by means of fundus photographs, OCT or FA) seems not to be fully adequate, mainly referring to therapeutic results (Browning et al. 2008). A more detailed classification of DME is obtained combining the information given by different diagnostic methods, as well as the future classification in different phenotypes. In this way, more customized treatment might give better functional results in patients with diabetes.

The described pattern of DME visualized by RM-SLO cannot be confused with other lesions as retinal pigment epithelium (RPE) changes, laser scars, most of which are depressions and not elevations on RM-SLO. But RM-SLO cannot distinguish the origin of macular oedema, mostly cystoid macular oedema.

A peculiar, and never previously reported, finding with RM-SLO is the visualization of leaking microaneurysms as localized elevations. These elevations correspond to microaneurysms that showed significant dye diffusion in late-phase FA (Fig. 4). In this way, RM-SLO, a fully non-invasive imaging technique, might give information currently obtained with invasive FA. However, FA remains the most important diagnostic tool in the evaluation of capillary nonperfusion in the macular area and changes in the perifoveal capillary ring, both accounting for visual acuity loss (Bresnick et al. 1984). The role of RM-SLO in the evaluation of ischaemic areas and leaking microanurysms (which appear similar to small drusen) need to be fully validated in an appropriate study. The major limitations of this study are the use of time instead of spectral domain OCT, which might have influenced the quantification of some smaller lesions. But, as previously mentioned, spectral domain OCT is not yet fully validated to

quantify the extension of DME. Another possible bias is attributed to the higher DME prevalence in population attending our tertiary clinical centres.

In conclusion, the combined use of purely non-invasive imaging tests might be sufficient in the evaluation of the presence and characteristics of DME. The role of FA, a well-known invasive technique, might be revisited as the diagnosis and follow-up of DME is concerned.

Acknowledgments

No funding/support was received for this study. The authors thank Fabiano Cavarzeran for the statistical analysis of data.

References

Acton JH, Cubbidge RP, King H, Galsworthy P & Gibson JM (2011): Drusen detection in retro-mode imaging by a scanning laser ophthalmoscope. Acta Ophthalmol **89**: 404–411.

Altman DG (1997): Practical Statistics for Medical Research. London: Chapman and Hall.

Bartsch DU, Weinreb RN, Zinser G & Freeman WR (1995): Confocal scanning infrared laser ophthalmoscopy for indocyanine green angiography. Am J Ophthalmol **120**: 642–651.

Beck RW, Edwards AR, Aiello LP et al. (2009): Diabetic Retinopathy Clinical Research Network (DRCR.net). Three-year follow-up of a randomized trial comparing focal/grid photocoagulation and intravitreal triamcinolone for diabetic macular edema. Arch Ophthalmol **127**: 245–251.

Bresnick GH, Condit R, Syrjala S, Palta M, Groo A & Korth K (1984): Abnormalities of the foveal avascular zone in diabetic retinopathy. Arch Ophthalmol **102**: 1286–1293.

Brown JC, Solomon SD, Bressler SB, Schachat AP, DiBernardo C & Bressler NM (2004): Detection of diabetic foveal edema: contact lens biomicroscopy compared with optical coherence tomography. Arch Ophthalmol **122**: 330–335.

Browning DJ, Altaweel MM, Bressler NM, Bressler SB & Scott IU (2008): Diabetic Retinopathy Clinical Research Network. Diabetic macular edema: what is focal and what is diffuse? Am J Ophthalmol **146**: 649–655.

Ehrlich R, Harris A, Ciulla TA, Kheradiya N, Winston DM & Wirostko B (2010): Diabetic macular oedema: physical, physiological and molecular factors contribute to this pathological process. Acta Ophthalmol **88**: 279–291.

Elsner AE, Burns SA, Hughes GW & Webb RH (1992): Reflectometry with a scanning laser ophthalmoscope. Appl Opt **31**: 3697–3710.

Elsner AE, Burns SA, Weiter JJ & Delori FC (1996): Infrared imaging of sub-retinal structures in the human ocular fundus. Vision Res **36**: 191–205.

Fawcett T (2006): An introduction to ROC analysis. Pattern Recogn Lett **27**: 861–874.

Hartnett ME & Elsner AE (1996): Characteristics of exudative age-related macular degeneration determined in vivo with confocal and indirect infrared imaging. Ophthalmology **103**: 58–71.

Holz FG, Bellmann C, Margaritidis M, Schütt F, Otto TP & Volcker HE (1999): Patterns of increased in vivo fundus autofluorescence in the junctional zone of geographic atrophy of the retinal pigment epithelium associated with age-related macular degeneration. Graefes Arch Clin Exp Ophthalmol **237**: 145–152.

Ikeda T, Sato K, Katano T & Hayashi Y (1998): Examination of patients with cystoid macular edema using a scanning laser ophthalmoscope with infrared light. Am J Ophthalmol **125**: 710–712.

Klein R, Klein BE, Moss SE & Cruickshanks KJ (1998): The Wisconsin Epidemiologic Study of Diabetic Retinopathy: XVII. The 14-year incidence and progression of diabetic retinopathy and associated risk factors in type 1 diabetes. Ophthalmology **105**: 1801–15.

McBain VA, Forrester JV & Lois N (2008): Fundus autofluorescence in the diagnosis of cystoid macular oedema. Br J Ophthalmol **92**: 946–949.

Ohkoshi K, Tsuiki E, Kitaoka T & Yamaguchi T (2010): Visualization of subthreshold micropulse diode laser photocoagulation by scanning laser ophthalmoscopy in the retro mode. Am J Ophthalmol **150**: 856–862.

Otani T, Kishi S & Maruyama Y (1999): Patterns of diabetic macular edema with optical coherence tomography. Am J Ophthalmol **127**: 688–693.

Pece A, Isola V, Holz F, Milani P & Brancato R (2009): Autofluorescence imaging of cystoid macular edema in diabetic retinopathy. Ophthalmologica **224**: 230–235.

Remky A, Beausencourt E, Hartnett ME, Trempe CL, Arend O & Elsner AE (1999): Infrared imaging of cystoid macular edema. Graefes Arch Clin Exp Ophthalmol **237**: 897–901.

Sim J & Wright CC (2005): The kappa statistic in reliability studies: use, interpretation, and sample size requirements. Phys Ther **85**: 257–268.

Virgili G, Menchini F, Dimastrogiovanni AF, Rapizzi E, Menchini U, Bandello F & Chiodini RG (2007): Optical coherence tomography versus stereoscopic fundus photography or biomicroscopy for diagnosing diabetic macular edema: a systematic review. Invest Ophthalmol Vis Sci **48**: 4963–4973.

Vujosevic S, Bottega E, Casciano M, Pilotto E, Convento E & Midena E (2010): Microperimetry and fundus autofluorescence in diabetic macular edema: subthreshold micropulse diode laser versus modified early treatment diabetic retinopathy study laser photocoagulation. Retina **30**: 908–916.

Vujosevic S, Casciano M, Pilotto E, Boccassini B, Varano M & Midena E (2011): Diabetic macular edema: fundus autofluorescence and functional correlations. Invest Ophthalmol Vis Sci **52**: 442–448.

Yamamoto M, Tsujikawa A, Mizukami S, Miyoshi N & Yoshimura N (2008): Cystoid macular edema in polypoidal choroidal vasculopathy viewed by a scanning laser ophthalmoscope: CME in PCV viewed by SLO. Int Ophthalmol **29**: 503–506.

Yamamoto M, Mizukami S, Tsujikawa A, Miyoshi N & Yoshimura N (2010): Visualization of cystoid macular oedema using a scanning laser ophthalmoscope in the retro-mode. Clin Experiment Ophthalmol **38**: 27–36.

Received on October 25th, 2011.
Accepted on January 23rd, 2012.

Correspondence:
Edoardo Midena, MD
Department of Ophthalmology
University of Padova
35128 Padova
Italy
Tel: + 390498212110
Fax: + 390498755168
Email: edoardo.midena@unipd.it